Applied Geomatics (2025) 17:401–410
https://doi.org/10.1007/s12518-025-00625-7

RESEARCH

Ensembling satellite monitoring and numerical cartography towards the safety assessment of infrastructures

Francesca Grassi[1] · Paolo Rossi[1] · Benedetta Brunelli[1,2] · Francesco Mancini[1] · Cristina Castagnetti[1] · Loris Vincenzi[1] · Elisa Bassoli[1] · Alessandro Capra[1]

Received: 25 February 2025 / Accepted: 19 March 2025 / Published online: 28 March 2025

Abstract
This paper explores new technologies that can advance the state-of-the-practice in safety assessment and health monitoring of existing infrastructures. In this context, multi-temporal interferometric Synthetic Aperture Radar techniques combined with the use of digital models of infrastructures represent a powerful integration to conventional approaches in the monitoring and assessment of structural safety of infrastructures. Although the interferometric method is widely used for ground deformation investigations, using displacement data from satellite observation in structural monitoring is less investigated. The joint use of multi-frequency satellite radar data provided by the European Space Agency Copernicus project and Italian Space Agency will be explored. The paper introduces the workflow implemented for processing satellite radar data from the X-band COSMO-SkyMed constellation by the Italian Space Agency over the municipality of Modena (Italy). An open-source workflow based on Multi-Temporal Interferometric technique and Persistent Scatterers Interferometry is adopted, enabling the detection of displacements of stable targets and the generation of corresponding time series. Radar data products, derived from the processing of both COSMO-SkyMed and Sentinel-1 data, are analyzed in a Geographic Information System alongside the available geospatial dataset of infrastructures. This approach enables the extraction of displacement components related to the ground and infrastructures. The method's potential for characterizing infrastructures behaviour is assessed through the analysis of selected case studies. The results aim to establish the foundations for a method capable of assessing infrastructure safety.

Keywords Persistent scatterer interferometry · Numerical cartography · Infrastructure safety assessment

✉ Paolo Rossi
paolo.rossi@unimore.it

Francesca Grassi
francesca.grassi94@unimore.it

Benedetta Brunelli
benedetta.brunelli@uniroma.it

Francesco Mancini
francesco.mancini@unimore.it

Cristina Castagnetti
cristina.castagnetti@unimore.it

Loris Vincenzi
loris.vincenzi@unimore.it

Elisa Bassoli
elisa.bassoli@unimore.it

Alessandro Capra
alessandro.capra@unimore.it

1 Department of Engineering "Enzo Ferrari", University of Modena and Reggio Emilia, Via Pietro Vivarelli 10, Modena 41125, Italy

2 Department of Civil, Constructional and Environmental Engineering, Sapienza - University of Rome, Via Eudossiana, 18, Rome 00184, Italy

Introduction

This study explores the potential of emerging technologies to enhance current practices in safety assessment and health monitoring of existing infrastructures. Traditional Structural Health Monitoring (SHM) techniques face several limitations, including high costs, resources demand, limited monitoring coverage and difficulties in accessing the structure (Gagliardi et al. 2023). Consequently, it is crucial to implement effective and innovative monitoring strategies for the predictive maintenance of these infrastructures. Such advancements aim to prevent deterioration processes and reduce the probability of structural failures. In this context, Multi Temporal Interferometric Synthetic Aperture Radar (MT-InSAR) techniques are able to ensure a wide, contactless and non-invasive monitoring of the mentioned infrastructures (Schlögl et al. 2022) providing long-term displacement data of coherent targets with millimeter-level accuracy and a high density of measurement points (Ferretti et al. 2001; Crosetto et al. 2016). Sentinel-1 (S1) by the European Space Agency (ESA) is a constellation part of the Copernicus project, which is the major ESA Earth Observation (EO) program, and it is composed of C-band SAR satellites providing complex data with worldwide coverage, an average spatial resolution and a short revisit time under a free and open access distribution policy. In the last years, a ground deformation service, the European Ground Motion Service (EGMS), was also implemented providing yearly updated S1 standardized ground motion products for the European territory (Crosetto et al. 2020). COSMO-SkyMed (CSK), the major EO Constellation by the Italian Space Agency (ASI), provides high resolution data and products for research, defense, risk management and commercial field (Covello et al. 2010) and it is composed by a first-generation X-band constellation of four satellites and a second-generation that is currently being completed to ensure the continuity to the first generation (Mari et al. 2018).

The benefits of the use of advanced SAR interferometric techniques in infrastructure monitoring are clear (Lazecky et al. 2016; Gagliardi et al. 2023); however, an in-depth analysis and integration between these techniques and traditional monitoring approaches need to be carried out. In particular, literature presents methods for the automatic or semi-automatic detection of potential instability from anomalous deformation by SAR data exploiting spatial and/or temporal analysis of mean velocities and displacement time series complemented by a validation with in-situ data or by a cross-validation with independent SAR datasets, even exploiting different operational frequencies (Zhu et al. 2018; Huang et al. 2018; Jung et al. 2019; Cusson et al., 2021; Schlögl et al. 2021). In addition, Nettis et al. (2023) proposed a method for the automatic interpretation of deformations of roads based on SAR data complemented by the assignment of a monitoring or priority class to infrastructures based on the detected deformation processes.

A review of the existing literature highlights the need for deeper integration of SAR-based products, traditional monitoring data and SHM methods relying on infrastructural digital models. To address this gap, we propose a procedure that combines multi-resolution SAR data with numerical cartography to characterize the behavior of infrastructures portions and analyze their different contributions to the occurring deformations. Specifically, to disentangle the different contributions to infrastructures deformation (in particular, the ground deformation and structural phenomena), S1 C-band data and CSK X-band are employed. Spatial analyses based on the dual-resolution SAR datasets and available numerical cartography about road network are conducted within a Geographic Information System (GIS) within the 183 km2 wide Municipality of Modena (Italy). The results are evaluated to assess the effectiveness of the method in the characterization of road infrastructures with successive in-depth analysis of selected case studies.

Data and methods

SAR dataset and numerical cartography

In this section, the available infrastructures geospatial dataset of the Municipality of Modena and the SAR dataset and products from S1 EGMS and CSK constellation are presented along with a brief description of the CSK data processing workflow.

Geospatial dataset

Open access geospatial data of infrastructures (i.e., roads and railways) of the Modena Municipality (Fig. 1) were downloaded from the geographic repository of the Emilia Romagna region (https://geoportale.regione.emilia-romagna.it/) and imported in a GIS environment. The layers representing the infrastructures include both geometric entities and descriptive attributes, such as construction type and operational status of each vector feature (polygons), upon which the analysis is based.

Sentinel-1 products by the European ground motion service (EGMS)

The S1 data used to depict the deformation trends are those acquired with the Interferometric Wide (IW) acquisition mode, which provides a spatial resolution of 5 m × 20 m (Geudtner et al. 2024), with successive analysis based on

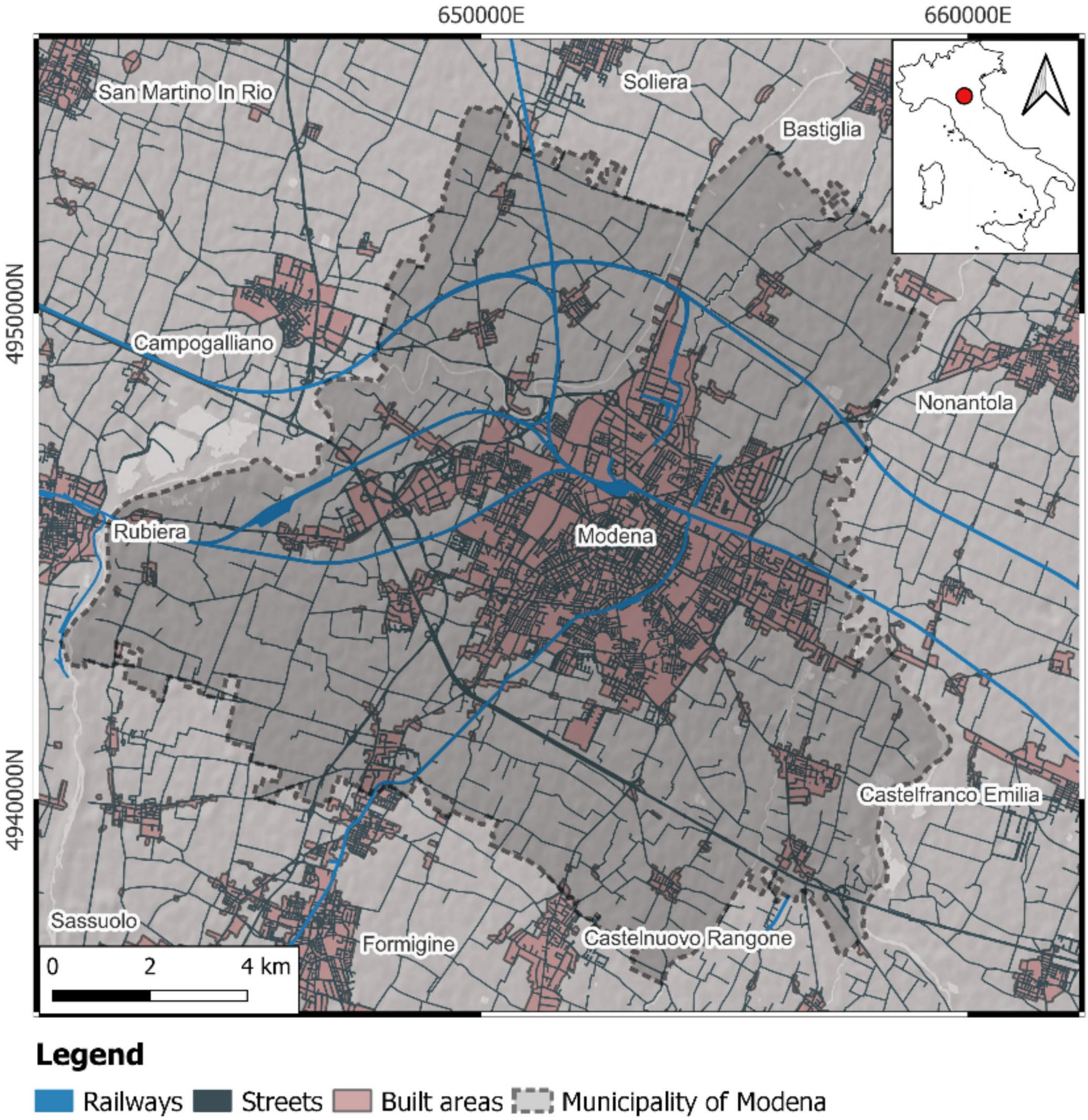

Fig. 1 The study area and the available geospatial datasets (background: ESRI Shaded Relief)

Persistent Scatterers Interferometry (PSI) approach as made available by EGMS. More in detail, the EGMS processing of S1 data is based on the combination of advanced multi-temporal interferometric techniques and high quality Global Navigation Satellite System (GNSS) models for calibration (Costantini et al. 2021). It provides the full-resolution Line-Of-Sight (LOS) oriented and calibrated time series of displacements, in addition to their components along the horizontal and vertical directions at resampled 100 m × 100 m spatial resolution.

The full resolution, calibrated and LOS-oriented products from a descending orbit over the municipality of Modena, were downloaded from the EGMS explorer (https://egms.land.copernicus.eu/) for a period spanning from 2015 to 2021 and imported in a GIS environment for successive analyses.

COSMO-SkyMed products by PSI processing

The CSK dataset used in this work consists of Single-look Complex Slant (SCS) Level 1 A descending data acquired with the Stripmap Himage mode (spatial resolution of 3 m × 3 m) spanning the years 2014–2018 and has been downloaded from the new ASI portal for Italian Institutional Users. The dataset was processed using open-source tools consisting in the ESA Sentinel Application Platform (SNAP) software, the Statistical Cost Network Flow Algorithm for Phase Unwrapping (SNAPHU) package (Chen and Zebker 2002), the Stanford Method for Persistent Scatterers (StaMPS) (Hooper et al. 2012), and MATLAB routines for calibration using GNSS data, as well as for exporting and analyzing the results (Mancini et al. 2021). Specifically, as illustrated in Fig. 2, the procedure yielded displacement time series and the average annual velocity for each coherent target (the Persistent Scatterers, PSs). Calibration was performed using GNSS data from the MOPS reference station, processed by the Nevada Geodetic Laboratory (Blewitt et al. 2018); the adopted GNSS processing strategy is able to retrieve velocities with an accuracy in the order of 1 mm/year or less (Blewitt et al. 2016). The calibration procedure involves the selection of a reference area in the vicinity of the GNSS calibration station and the identification of PS targets within this area. Subsequently, the GNSS velocities are projected along the SAR line of sight (v_{LOS}) and computed as:

$$v_{LOS} = v_{UP}\cos\theta_{INC} - \sin\theta_{INC}\left[V_N\cos\left(\alpha_H - \frac{3\pi}{2}\right) + v_E\sin\left(\alpha_H - \frac{3\pi}{2}\right)\right] \quad (1)$$

In which v_{UP}, v_N, and v_E represent the GNSS velocities along the vertical, North-South, and East-West directions, respectively, θ_{INC} denotes the incidence angle and α_H is the heading angle. The associated level of uncertainty ($\sigma_{V,LOS}$) is computed from Eq. (1) through an uncertainty propagation procedure based. Subsequently, the mean velocity of the selected PS LOS velocities is computed and aligned with the LOS-projected GNSS velocity, ensuring that the entire PS dataset is adjusted accordingly. This step introduces a constraint to a global reference frame.

The calibration procedure may affect the overall uncertainty of the results; its impact can be quantified through an error propagation analysis, incorporating the uncertainties affecting both the PSs and the GNSS data. As demonstrated by Mancini et al. (2021), the proposed workflow complemented by the calibration procedure is able to retrieve PS calibrated vertical and horizontal velocities after decomposition, which exhibit a discrepancy of less than 2 mm/yr with respect to independent GNSS validation site velocities, with levels of uncertainty that are, in the majority of cases, less than 1–2 mm/yr.

Analysis of multi-resolution SAR data and numerical cartography

The joint analysis of multi-resolution SAR products and numerical cartography of road assets in the Municipality of Modena was conducted using QGIS software (version 3.22.12). The main steps of the analysis include: (1) collection and selection of SAR and GIS data, (2) defining an infrastructure layer consisting of polygons and specific dynamic buffers and determining ground displacement

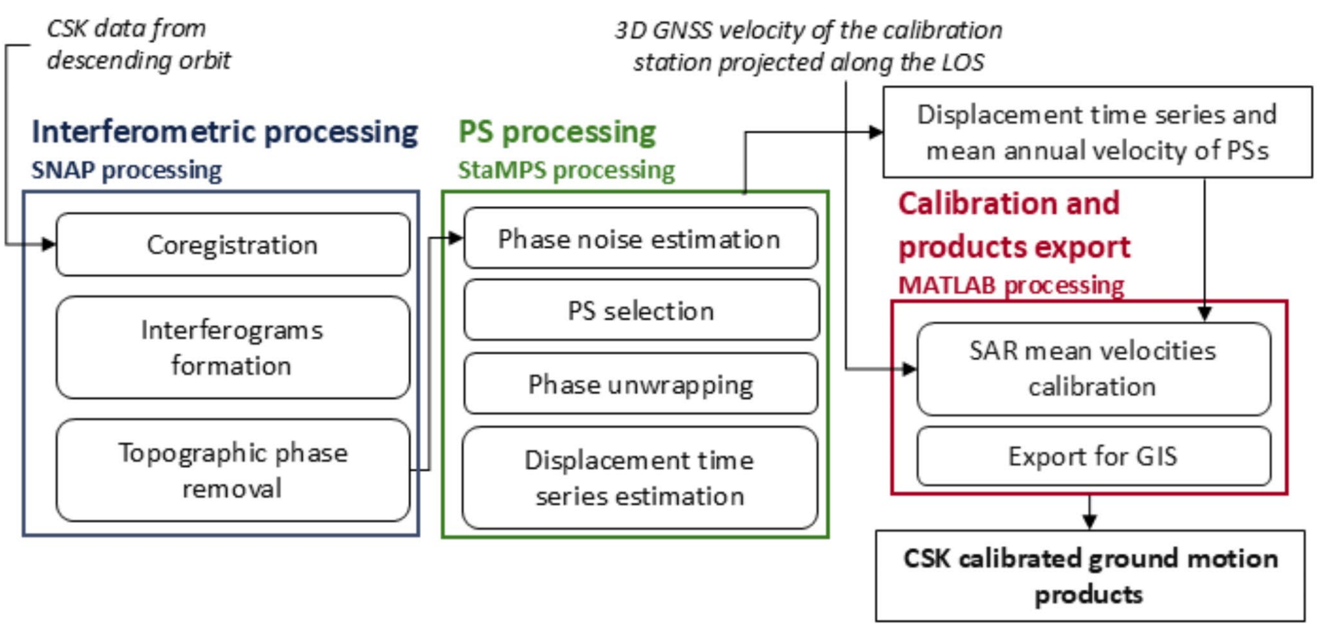

Fig. 2 PSI processing of the CSK dataset. (modified from Parenti et al. 2024)

using interpolated S1 products, (3) determining the global infrastructures displacement through CSK ground motion products, (4) analyzing the different contribution to the infrastructures displacement to characterize the behavior of each vector feature representing road infrastructure and (5) evaluating the results to assess the potentialities of the method in the structural characterization and in-depth analysis of selected case studies. A detailed outline of the methodology is presented in Fig. 3.

Results and discussions

The results from the analyses described in Sect. "Analysis of multi-resolution SAR data and numerical cartography" and illustrated in Fig. 3 are presented in this Section, with a focus on two representative case studies. While the same analyses were performed for both railways and the road infrastructure layers, only the results related to the railway infrastructures are reported in this section to ensure clarity and conciseness in the presentation.

First, we analyzed the railway infrastructure within the municipality of Modena, comprising a total of 196.3 km of railways (ALL), represented by 420 polygons in the GIS layer. Out of this total, 165 km correspond to ordinary railway infrastructure (ORD), while 31 km belong to high-speed railway infrastructure (HS). Among the ordinary lines, 91% of the length lies on the ground level (referred to as GRD), 48% refers to viaducts/overpasses/bridges (RSD), and 4.1% to tunnels (later TNL). For the high-speed railway lines, 25.8% of the length is at ground level (GRD), while 74.2% is on viaduct or similar elevated structures (RSD).

The initial analysis of the proposed methodology involved the railway segments where a sufficient amount of data were available. To this end, only polygons with more than three PSs (denoted as >3) were included in the stability analysis. This threshold was selected as the minimum required to obtain reliable average values for displacement. Notably, the actual number of PSs for each polygon typically exceeds this threshold, with ordinary railway polygons averaging 41 PSs, and high-speed railway polygons averaging 407 PSs.

The velocity analysis was conducted considering both the railway type (ORD and HS) and the construction type of specific segments (i.e., at ground level, on viaducts/overpasses/bridges, or in tunnels). Overall, 62% of the polygons representing the entire railway network were detected (ALL>3), comprising 60.5% of ordinary railway lines (ORD>3) and 91.3% of high-speed railway lines (HS>3). In terms of total railway length, the methodology detected the 89%, including 87% of ORD lines and 99.8% of HS lines. Regarding construction types, the method detected 86.7% of ground-level lines and nearly 100% of viaduct/overpass/bridge segments and tunnel segments for both ORD and HS railway categories. A summary of the results is provided in Table 1.

Analysis of the CSK-derived (global) velocities for the polygons of Table 1 denoted as ">3" reveals that all infrastructure segments, including both ordinary and high-speed railway lines, exhibit an overall global mean velocity (i.e., from CSK processing) greater than 2 mm/year away from the satellite (i.e., -2 mm/year).

To isolate the contribution of infrastructures behaviour to the overall velocity, the difference between the global (from CSK processing) and the ground (obtained from S1 EGMS interpolated and reprojected ground motion products after excluding those belonging to infrastructure) velocities was computed. This difference represents the residual motion component affecting the infrastructure potentially linked to localized phenomena. Infrastructures segments exceeding a given threshold can be easily identified as priority areas requiring further analysis. For this analysis, a threshold of 4 mm/year was applied accounting for the uncertainties affecting the mean velocities derived from S1 and CSK PSI processing through uncertainty propagation.

The results indicate:

- for ordinary railway lines (ORD>3), 27% of the ground-level segments, 29% of the elevated, and 4% of the tunnels exhibit velocities exceeding the set threshold.
- for high-speed railway lines (HS>3), 100% of the ground-level segments, and 44% of the elevated display velocities above the set threshold.

These findings highlight the need for targeted investigations in specific segments to address potential localized phenomena affecting structural stability. Among the selected infrastructures segments, two representative examples have been chosen for detailed analysis. Figure 4 illustrates a section of an ordinary railway line, which includes polygons classified as both "raised" and "at ground level". Figure 5 presents two examples of a high speed railway line. The overall velocities affecting the infrastructures, represented by the CSK calibrated mean annual velocities, are shown in Figs. 4a and 5 HS1-a and 5 HS2-a. The velocity components associated exclusively with the infrastructure portions, referred to as residual velocities, are displayed in Figs. 4b and 5 HS1-b, and 5 HS2-b.

Figure 4 depicts an area where a ground subsidence of 2–4 mm/year has been computed based on the interpolation of S1 ground motion products. The analysis of the differences (Fig. 4b) between the ground subsidence and the global deformation (Fig. 4a) reveals that nearly all portions

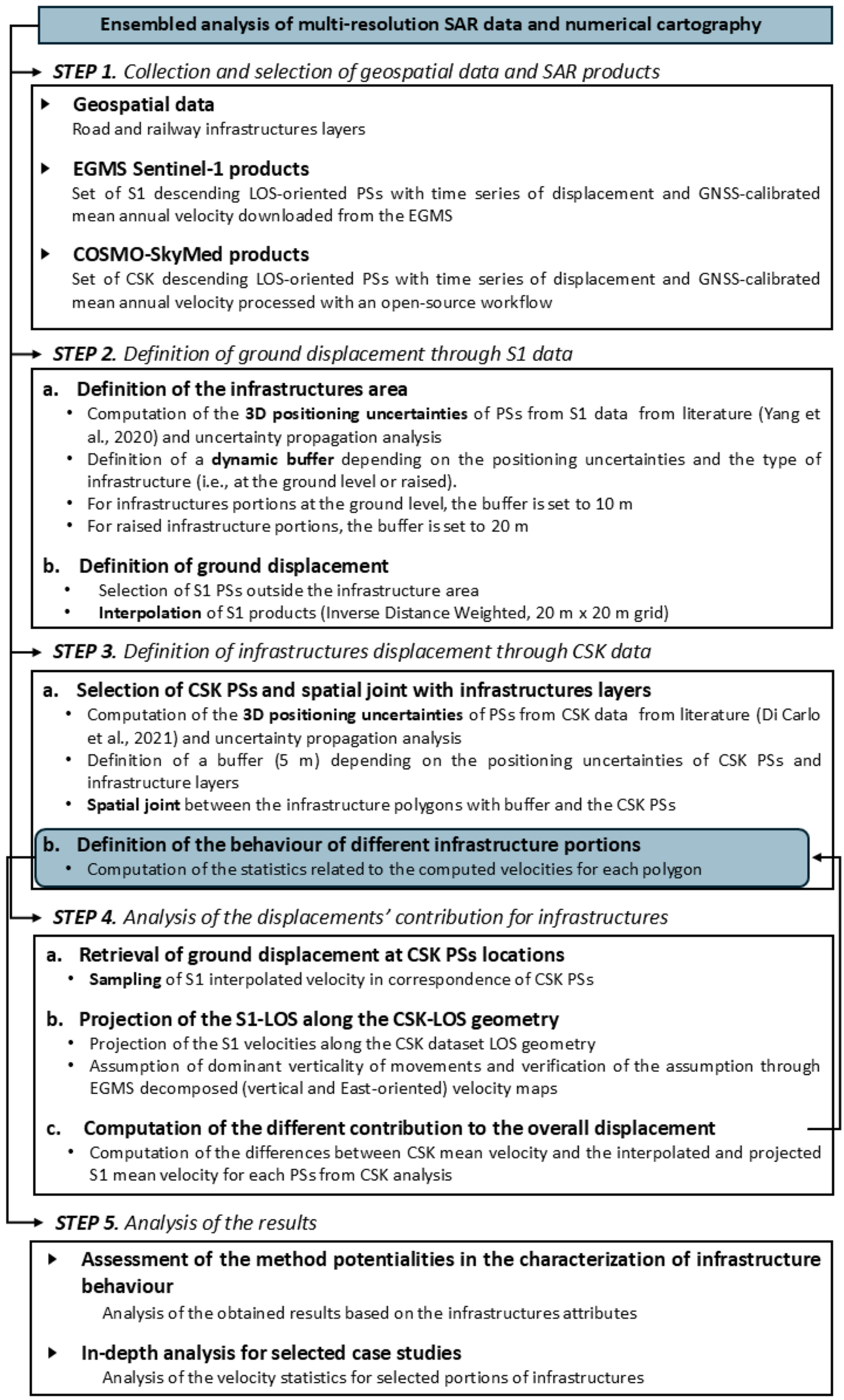

Fig. 3 The analysis of multi-resolution SAR data and numerical cartography

Table 1 Method's ability in the detection of different railway types (ORD and HS) and construction types (GRD, RSD, TNL). Absolute values (in terms of length and number of polygons with more than 3 PSs) and corresponding percentages are summarized

Railway	Polygons #	Polygons %	Length [km]	Length %
ALL	420		196.3	
ALL>3	261	62 of ALL	174.7	89 of ALL
ORD	397		165.3	
GRD	358	90.2 of ORD	150.4	91 of ORD
RSD	28	7.0 of ORD	7.9 of ORD	4.8 of ORD
TNL	11	2.8 of ORD	6.8	4.1 of ORD
ORD>3	240	60.5 of ORD	143.8	87 of ORD
GRD>3	215	89.6 of ORD>3	129.5	90 of ORD>3
RSD>3	17	7.1 of ORD>3	8	5.4 of ORD>3
TNL>3	8	3.3o f ORD>3	6.6	4.6 of ORD>3
HS	23		31	
GRD	13	56.5 of HS	8	25.8 of HS
RSD	10	43.5 of HS	23	74.2 of HS
HS>3	21	91.3 of HS	30.9	99.8 of HS
GRD>3	11	52.4 of HS>3	7.9	25.6 of HS>3
RSD>3	10	47.6 of HS>3	23	74.4 of HS>3

of the ordinary railway are affected by residual phenomena impacting the infrastructure. In particular, the ground-level segments exhibit a residual negative annual velocity ranging from 10 to 16 mm/year, which accounts for approximately 80% of the global velocity affecting these infrastructure segments.

These findings suggest that the structure and the generation process of the available geospatial dataset play a crucial role in the proposed analysis. Given that the average polygon length is 416 m for ordinary railways and 1.35 km for high-speed railways, the behavior of selected high-speed infrastructures segments may not be adequately captured by the developed method.

The issue related to polygon length is further highlighted in Figs. 5 HS1 and HS2. Some portions of the high-speed railway line at ground level are affected by global motion components whose magnitude varies along their length. In the case presented in Fig. 5 HS1, the polygons in the numerical cartography are sufficiently detailed to capture the spatial variability of the phenomenon. As a result, the method effectively identifies specific portions that may be prone to stability issues. Conversely, Fig. 5 HS2 illustrates the limitation introduced by a coarser subdivision of polygons in the numerical cartography. In this case, despite the high density of PSs which could accurately describe the spatial evolution of the phenomenon, the excessive length of the available polygon prevents a precise identification of infrastructures sections susceptible to potential criticalities.

In light of these results, a finer subdivision of the polygons would enhance the representation of the behavior of specific infrastructure segments. However, this largely depends on the characteristics of the existing numerical cartography, which is not designed to capture such detailed aspects of infrastructure at this level of precision.

Moreover, recent methods for analyzing displacements identified through PS-InSAR allow for overcoming the aforementioned limitations related to the low resolution of numerical cartography. These methods rely on the analysis of the 2D spatial gradient of PS velocities, an approach that can enhance the reconstruction of the spatial characteristics of the phenomenon. In this context, Shahbazi et al. (2024) recently proposed a method for detecting buildings with potential damage based on differential deformation maps generated from the PSs velocities gradient. Specifically, the authors compute the spatial velocity gradient from SAR-based PS velocities associated with buildings polygons and classify them based on the maximum spatial deformation observed for each building. The method has been tested using both S1 and CSK datasets to generate differential deformation map for buildings. However, with appropriate modification, such as refining the selection of PSs associated with infrastructure polygons and adjusting the classification criteria based on velocity gradient, this approach could be applied to our study to improve the understanding of deformations affecting different infrastructure segments.

In this scenario, new perspectives are also offered by Building Information Modeling (BIM) approaches towards a more complete and deep description of structures and infrastructures. BIM provides a more comprehensive and effective framework for monitoring and designing activities. A detailed geometric description of the infrastructure, complemented by structural information, would enable a more precise characterization of the structure and its behaviour. Furthermore, the availability of a digital twin of the infrastructure would provide an advanced representation to be used as a reference model for the integrated use of geometrical, structural and monitoring data.

Conclusions

In this paper, a method based on the ensembled analysis of multi-resolution SAR deformation products and numerical cartography to enhance the current practices in safety assessment and health monitoring of infrastructures is proposed.

The deformation affecting the entire territory of the Municipality of Modena (Italy) is retrieved by S1 EGMS ground deformation products. After interpolation and reprojection onto the CSK-LOS geometry, the ground subsidence affecting the infrastructures is computed. This component is then compared with the global one affecting the infrastructures, derived from CSK data PSI processing, to identify the residual phenomena specifically affecting the portions of the

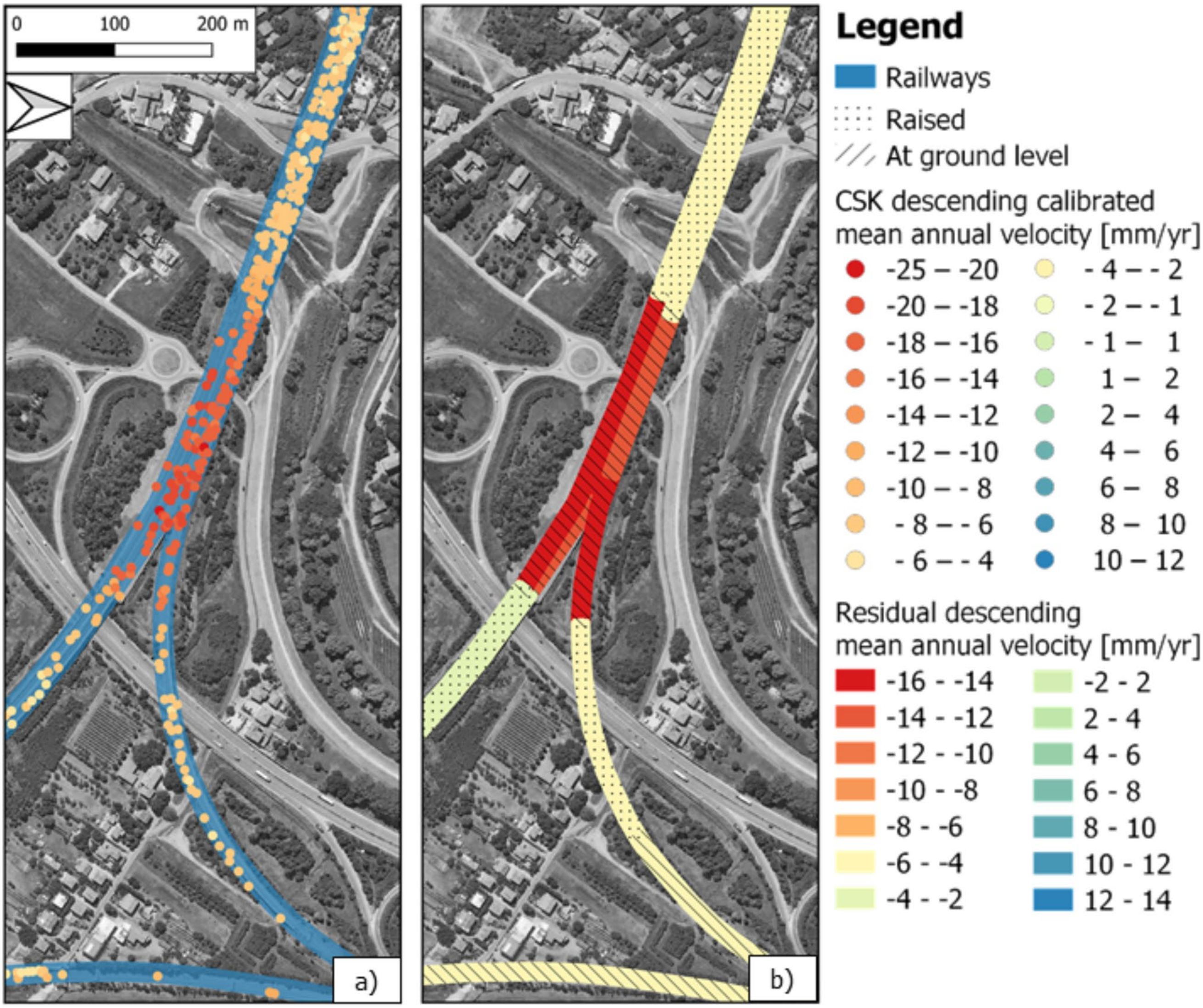

Fig. 4 Ordinary railway portion in the Municipality of Modena: **a**) infrastructures global velocities derived from CSK data, **b**) infrastructures residual velocity obtained by calculating the difference between S1 interpolated (ground) and CSK data (background: Google Satellite)

infrastructures. The different motion contributions are analyzed in relation to the construction type of infrastructures, as provided by the available geospatial dataset, to select infrastructure portions exhibiting residual components. The results demonstrate that the method can detect most of the infrastructures (87% of the total length for the ordinary railway and 99.8% for the high-speed railway), regardless of construction type.

The proposed methodology can also be effectively applied to other structures of interest, such as roads and buildings (Grassi et al. 2022) and it is adaptable to locations beyond the presented case study. However, its applicability is subjected to certain limitations, primarily related to the availability of a sufficient density of satellite radar targets (e.g., areas with low vegetation cover), the ability of radar data to retrieve the occurring displacements and the availability of geospatial datasets with sufficient attributes. A key factor of the proposed method is the vectorization approach used for geospatial datasets. In the Modena case study, the INSPIRE directive (Infrastructure for Spatial Information in Europe – Directive 2007/2/EC) is adopted, which applies consistently across Italy and Europe. More detailed and accurate analyses can be achieved when vectorization is highly precise in terms of both geometry (small vectors and polygons) and attribute information (rich and detailed attribute sets). Moreover, recently proposed methods based on the analysis of the 2D spatial PS velocity gradient (Shahbazi et al. 2024) could enhance the reconstruction of the spatiality of the phenomenon.

In this study, the analysis of the computed velocities and different motion contributions has enabled to preliminary reconstruct the behavior of the railway infrastructure

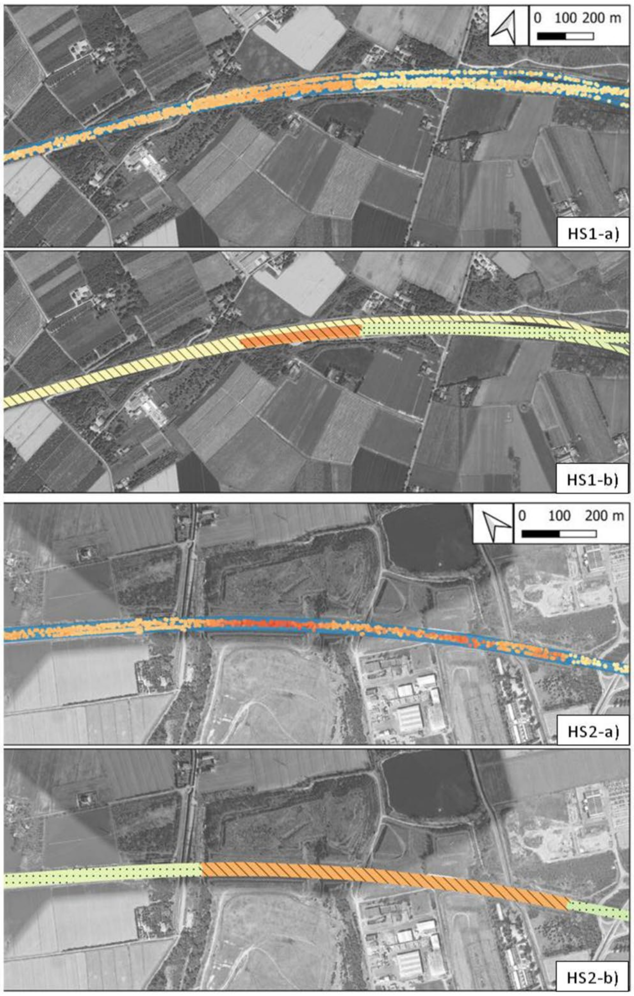

Fig. 5 High speed railway segments in the Municipality of Modena: HS1/HS2-a) infrastructures global velocities from CSK data, HS1/HS2-b) infrastructures residual velocity calculated as the difference between S1 interpolated (ground) and CSK data (refer to Fig. 4 for the legend; background: Google Satellite)

segments; to further enhance the analysis, additional efforts should be focused on providing a more detailed and comprehensive description of the infrastructure's portions. In this regard, emerging approaches based on BIM could be particularly beneficial, especially for the integration of geometric and monitoring data in the context of a more innovative and effective safety assessment methodology.

Acknowledgements Project carried out using COSMO-SkyMed Products, © of the Italian Space Agency (ASI), delivered under a license to use by ASI.

Author contributions Conceptualization, GF, FM, RP; methodology, GF, MF. RP; data processing, GF; first draft, GF, RP; review and editing, ALL; and study supervision MF, CC, CA.

Funding Open access funding provided by Università degli Studi di Modena e Reggio Emilia within the CRUI-CARE Agreement.
The presented research was funded by the Project "Damage Analysis and Monitoring of Ancient structures interacting with Geotechnical Excavations (DAMAGE)" PIANO NAZIONALE DI RIPRESA E RESILIENZA (PNRR) – Missione 4 – Componente 2. Dalla Ricerca all'Impresa -Investimento 1.1 Fondo per il Programma Nazionale della Ricerca (PNR) e Progetti di Ricerca di Rilevante Interesse Nazionale (PRIN), finanziato dall'Unione europea – NextGenerationEU - rif. D.D. N. n. 104 del 02/02/2022 (CUP: E53D23002550006; cod. Progetto 20222M8E9A).

Data availability Numerical cartography is available at: https://geoportale.regione.emilia-romagna.itSentinel products by EGMS are available at: https://egms.land.copernicus.euCOSMO-SkyMed data are delivered under a license to use by ASI (Agenzia Spaziale Italiana).

Declarations

Competing interests The authors declare no competing interests.

References

Blewitt G, Kreemer C, Hammond WC, Gazeaux J (2016) MIDAS robust trend estimator for accurate GPS station velocities without step detection. J Geophys Research: Solid Earth 121:2054–2068. https://doi.org/10.1002/2015JB012552

Blewitt G, Hammond W, Kreemer C (2018) Harnessing the GPS data explosion for interdisciplinary science. Eos 99(2):e2020943118

Chen CW, Zebker HA (2002) Phase unwrapping for large SAR interferograms: statistical segmentation and generalized network models. IEEE Trans Geosci Remote Sens 40(8):1709–1719. https://doi.org/10.1109/TGRS.2002.802453

Costantini M, Minati F, Trillo F, Ferretti A, Novali F, Passera E,… and, Andersen HS (2021) European ground motion service (EGMS). IEEE international geoscience and remote sensing symposium IGARSS (pp. 3293–3296)

Covello F, Battazza F, Coletta A, Lopinto E, Fiorentino C, Pietranera L,… and, Zoffoli S (2010) COSMO-SkyMed an existing opportunity for observing the Earth. J Geodyn 49(3–4):171–180. https://doi.org/10.1109/IGARSS47720.2021.9553562

Crosetto M, Monserrat O, Cuevas-González M, Devanthéry N, Crippa B (2016) Persistent scatterer interferometry: A review. ISPRS J Photogrammetry Remote Sens 115:78–89. https://doi.org/10.1016/j.isprsjprs.2015.10.011

Crosetto M, Solari L, Mróz M, Balasis-Levinsen J, Casagli N, Frei M,… and, Andersen HS (2020) The evolution of wide-area DInSAR: From regional and national services to the European Ground Motion Service. Remote Sensing, 12(12):2043. https://doi.org/10.3390/rs12122043

Cusson D, Rossi C, Ozkan IF (2021) Early warning system for the detection of unexpected Bridge displacements from radar satellite data. J Civil Struct Health Monit 11(1):189–204. https://doi.org/10.1007/s13349-020-00446-9

Ferretti A, Prati C, Rocca F (2001) Permanent scatterers in SAR interferometry. IEEE Trans Geosci Remote Sens 39(1):8–20. https://doi.org/10.1109/36.898661

Gagliardi V, Tosti F, Bianchini Ciampoli L, Battagliere ML, D'Amato L, Alani AM, Benedetto A (2023) Satellite remote sensing and non-destructive testing methods for transport infrastructure monitoring: advances, challenges and perspectives. Remote Sens 15(2):418. https://doi.org/10.3390/rs15020418

Geudtner D, Torres R, Snoeij P, Davidson M, Rommen B (2024) Sentinel-1 system capabilities and applications. In 2014 IEEE geoscience and remote sensing symposium (pp. 1457–1460). https://doi.org/10.1109/IGARSS.2014.6946711

Grassi F, Mancini F, Bassoli E, Vincenzi L (2022) Contribution of anthropogenic consolidation processes to subsidence phenomena from multi-temporal DInSAR: a GIS-based approach. GIScience Remote Sens 59(1):1901–1917. https://doi.org/10.1080/15481603.2022.2143683

Hooper A, Bekaert D, Spaans K, Arıkan M (2012) Recent advances in SAR interferometry time series analysis for measuring crustal deformation. Tectonophysics 514:1–13. https://doi.org/10.1016/j.tecto.2011.10.013

Huang Q, Monserrat O, Crosetto M, Crippa B, Wang Y, Jiang J, Ding Y (2018) Displacement monitoring and health evaluation of two bridges using Sentinel-1 SAR images. Remote Sens 10(11):1714. https://doi.org/10.3390/rs10111714

Jung J, Kim DJ, Palanisamy Vadivel SK, Yun SH (2019) Long-term Deflection monitoring for bridges using X and C-band time-series SAR interferometry. Remote Sens 11(11):1258. https://doi.org/10.3390/rs11111258

Lazecky M, Hlavacova I, Bakon M, Sousa JJ, Perissin D, Patricio G (2016) Bridge displacements monitoring using space-borne X-band SAR interferometry. IEEE Journal of Selected Topics in Applied Earth Observations and Remote Sensing, 10(1), 205–210. 10. https://doi.org/10.1109/JSTARS.2016.2587778

Mancini F, Grassi F, Cenni N (2021) A workflow based on SNAP–StaMPS open-source tools and GNSS data for PSI-Based ground deformation using dual-orbit sentinel-1 data: accuracy assessment with error propagation analysis. Remote Sens 13(4):753. https://doi.org/10.3390/rs13040753

Mari S, Valentini G, Serva S, Scopa T, Cardone M, Fasano L, De Luca GF (2018) COSMO-SkyMed second generation system access portfolio. IEEE Geoscience Remote Sens Magazine 6(1):35–43. https://doi.org/10.1109/IGARSS.2016.7729532

Nettis A, Massimi V, Nutricato R, Nitti DO, Samarelli S, Uva G (2023) Satellite-based interferometry for monitoring structural deformations of Bridge portfolios. Autom Constr 147:104707. https://doi.org/10.1016/j.prostr.2023.01.255

Parenti C, Grassi F, Rossi P, Soldati M, Pattuzzi E, Mancini F (2024) Synergistic use of synthetic aperture radar interferometry and Geomorphological analysis in Slow-Moving landslide investigation in the Northern apennines (Italy). Land 13(9):1505. https://doi.org/10.3390/land13091505

Schlögl M, Widhalm B, Avian M (2021) Comprehensive time-series analysis of Bridge deformation using differential satellite radar interferometry based on Sentinel-1. ISPRS J Photogrammetry Remote Sens 172:132–146. https://doi.org/10.1016/j.isprsjprs.2020.12.001

Schlögl M, Dorninger P, Kwapisz M, Ralbovsky M, Spielhofer R (2022) Remote sensing techniques for Bridge deformation monitoring at millimetric scale: investigating the potential of satellite radar interferometry, airborne laser scanning and ground-based mobile laser scanning. PFG–Journal Photogrammetry Remote Sens Geoinf Sci 90(4):391–411. https://doi.org/10.1007/s41064-022-00210-2

Shahbazi S, Barra A, Gao Q, Crosetto M (2024) Detection of buildings with potential damage using differential deformation maps. ISPRS J Photogrammetry Remote Sens 218:57–69. https://doi.org/10.1016/j.isprsjprs.2024.10.008

Zhu M, Wan X, Fei B, Qiao Z, Ge C, Minati F,… and, Costantini M (2018) Detection of Building and infrastructure instabilities by automatic Spatiotemporal analysis of satellite SAR interferometry measurements. Remote Sens 10(11):1816. https://doi.org/10.3390/rs10111816